ISTITUTO NAZIONALE DI FISICA NUCLEARE

Sezione di Trieste

INFN/AE-91/12

17 Settembre 1991

C. Bortolotto, G. Cosmo, A. De Angelis, P. Eerola, J. Kalkkinen and A. Linussio

A MEASUREMENT OF THE PARTIAL HADRONIC WIDTHS OF THE Z^0 USING NEURAL NETWORKS

Servizio Documentazione
dei Laboratori Nazionali di Frascati

A MEASUREMENT OF THE PARTIAL HADRONIC WIDTHS OF THE Z^0 USING NEURAL NETWORKS

C. Bortolotto, G. Cosmo, A. De Angelis and A. Linussio
Istituto di Fisica dell'Universita' di Udine and INFN Trieste
Via Fagagna 208, 33100 Udine, Italy

P. Eerola[1] and J. Kalkkinen[2]
Dept. of High Energy Physics, University of Helsinki
Siltavuorenperger 20 C, SF-00170 Helsinki 17

To be published in the proceedings of the **Workshop on Neural Networks: from Biology to High Energy Physics**, Isola d'Elba (Italy), June 1991.

ABSTRACT

From the data collected by the DELPHI detector at LEP during 1990, the hadronic branching fractions of the Z^0 boson into all five known quarks have been measured for the first time in the literature.

A classifier based on a feed-forward neural network has been used for separating the hadronic decays of the Z^0 into four classes, corresponding to $(u\bar{u}+d\bar{d})$ unresolved, $s\bar{s}$, $c\bar{c}$, $b\bar{b}$. Data on the hard final-state photon radiation have been then used to resolve the decay rate into $u\bar{u}$ pairs from the decay rate into $d\bar{d}$ pairs.

The preliminary results are consistent with the predictions from the Standard Model. Problems related to the estimate of systematics are discussed.

1. INTRODUCTION

Measurements of the partial widths of the Z^0 into charged leptons were available from LEP since 1989, and presently the relative accuracy on their determination is of the order of 1% [1]. Despite the primary importance of the knowledge of the hadronic branching fractions, after two years of running of LEP, only the partial widths into $b\bar{b}$ pairs and into $c\bar{c}$ pairs have been measured, with accuracies in the range $5-10\%$ and $10-20\%$ respectively [2]. The lack of experimental information in the hadronic sector is mainly due to the difficulty of separating events in which the Z^0 decays into a pair of light quarks.

A powerful probe for the classification of events can be given by feed-forward neural networks [3], that can map a set of variables calculated from the topology of

[1]Now at CERN, Geneva, Switzerland.
[2]From SEFT. Visitor at the Institute of Physics of the University of Udine.

the event onto a feature space in which the different species are well separated. The possibility of using a feed-forward neural network for this purpose was explored in [4], for the problem of the classification of decays into $b\bar{b}$ pairs. The result of this study was that, in the case of a perfect detector, a separation could be achieved with a higher efficiency with respect to traditional separation variables [5]. Further studies [6] demonstrated that, also in the presence of detector effects, feed-forward neural networks could be a useful tool for the classification of $b\bar{b}$ events.

In what follows it is tested wether topological properties of the event (i.e., properties related to the structure of multiparticle production) can be used by a feed-forward neural network to classify not only $b\bar{b}$ events, but also $s\bar{s}$, $c\bar{c}$ and $(u\bar{u}+d\bar{d})$ unresolved events. The robustness of the separation against a wide range of systematic uncertainties related to the model-dependence of the classification has been investigated. As a result, it has been possible to measure, from the data collected by the DELPHI detector [7] at LEP during 1990, the rates of the hadronic decays into the four classes listed above.

For the sake of completeness, the LEP measurements of the rate of final state radiation from $q\bar{q}$ pairs have been used to compute the relative probabilities of decay into $u\bar{u}$ and $d\bar{d}$ pairs. This last separation is based on the assumption that the absolute value of the charge of the u quark is double with respect to the absolute value of the charge of the d quark, and thus, the probability for the photon bremsstrahlung process is four times larger.

2. EXPERIMENTAL PROCEDURE AND EVENT SAMPLE

This analysis is based on a data sample collected by the DELPHI detector at LEP during 1990.

The components of the DELPHI detector, relevant for this analysis, have already been described in Ref. [8], as well as the trigger for the hadronic events.

Charged tracks are measured in a 1.2 Tesla magnetic field by a set of three cylindrical tracking detectors : the Inner Detector (ID) (inner radius = 12 cm, outer radius = 28 cm, covering polar angles between 29^0 and 151^0), the Time Projection Chamber (TPC) (inner radius = 30 cm, outer radius = 122 cm, covering polar angles between 21^0 and 159^0) and the Outer Detector (OD) (inner radius = 198 cm, outer radius = 206 cm, covering polar angles between 42^0 and 138^0).

TPC, ID and OD provide a complete coverage of the region between 25° and 155° in the polar angle θ, with reconstruction efficiency near to 1. The average momentum resolution is $\Delta p/p \simeq 0.005\ p$ (p in GeV/c).

Only charged particles fulfilling the following criteria were used in the analysis: (a) impact parameter at the nominal primary vertex below 5 cm in radius from the beam axis and to within 10 cm of the nominal crossing point in z; (b) momentum p larger than 0.1 GeV/c; (c) measured track length in TPC above 50 cm; (d) polar angle θ between 25° and 155°.

All particles were assumed to be pions. Hadronic events were then selected by

requiring that: (a) each of the two hemispheres $cos\theta < 0$ and $cos\theta > 0$ contained a total energy of the charged particles $E_{ch} = \Sigma E_i$ larger than 3 GeV, where E_i are the particle energies; (b) the total energy of the charged particles seen in both hemispheres together exceeded 15 GeV; (c) there were at least 5 charged particles with momenta above 0.2 GeV/c; (d) the polar angle θ of the sphericity axis was in the range $40° < \theta < 140°$ (this cut ensures that the retained events were well contained inside the TPC).

The resulting data sample contains 79015 hadronic events. The contamination from beam-gas scattering, $\gamma\gamma$ interactions and $\tau^+\tau^-$ events is negligible ($< 0.3\%$).

3. VARIABLES USED FOR THE SEPARATION

Eighteen variables were used as an input for the separation.

Their choice came from the examination of the literature, and from a study of flavour-dependent distributions based on the JETSET 7.2 Parton Shower Monte Carlo [9] (JETSET PS in the following), that has proven, after two years of activity of LEP, to reproduce well the main features of the hadronic decays of the Z^0 [8, 10]. The particles in the event were clustered in jets according to the JADE/E0 algorithm [11], with $y_{cut} = 0.05$. In the following, the most energetic jet will be called "first jet", and indicated by the superscript (f); the second most energetic jet will be called "second jet", and indicated by the superscript (s).

The variables used are:

1. The sphericity $S^{(f)}$ of the first jet, calculated after a boost $\beta = 0.96$ along its axis. The axis of the jet was defined by the sum of the momenta of the particles belonging to it.

2. The directed sphericity $S^{(f)}_{1234}$ of the 4 most energetic particles in the first jet. For a set Q of tracks in a jet, this variable is defined as

$$S_Q = \frac{\sum_Q p_t^2}{\sum_Q |p|^2}$$

   where the $|p|$'s are the momenta in the rest frame of the set Q and the p_t's are their components perpendicular to the original jet direction in the laboratory frame.

3. The directed sphericity $S^{(s)}_{1234}$.

4. The invariant mass $M^{(f)}_{1234}$ of the 4 most energetic particles in the first jet.

5. The invariant mass $M^{(s)}_{1234}$ of the 4 most energetic particles in the second jet.

6..9. The products of the homologue direct sphericities for triplets of particles in the first and second jet, $S^{(f)}_{ijk} \times S^{(s)}_{ijk}$.

10..13. The products of the homologue invariant masses for triplets of particles in the first and second jet, $M^{(f)}_{ijk} \times M^{(s)}_{ijk}$.

14. The momentum of the slowest pion of the jet 1, after a boost along the jet axis corresponding to a D^* energy equal to one half of the beam energy.

15. Same as 14., for the second jet.

16. The momentum of the most energetic K^0 in the event (0 if no kaons reconstructed).

17. The momentum component perpendicular to the axis of the nearest jet of the most energetic K^0 in the event (0 if no kaons reconstructed).

18. The sum over the jets of the ratios between the momentum of the leading particle and the momentum of the jet.

All variables were rebinned in such a way that they were ranging from 0 to 1. Examples of the distributions of the variables can be seen in Fig. 1, compared with a simulation based on JETSET PS plus the full detector simulation DELSIM [12].

4. THE NEURAL NETWORK CLASSIFIER

Four independent feed-forward neural networks have been used (one for each class that had to be separated) with 18 nodes in the input layer, associated with the input variables x_i, defining the pattern space P; a variable number of nodes in the hidden layer; and one output node, associated with the output value Θ, belonging to the feature space F. The number of nodes in the hidden layer of each network was chosen by making different trials with an increasing number of nodes, and stopping when the classification efficiency was reaching a plateau.

In the structure chosen, each neuron (node) performs a weighted sum of the output values from all the nodes of the previous layer; the node output is then computed via a sigmoid function

$$g_T(x) = \frac{1}{1 + e^{-x/T}}$$

at a "temperature" T[3]. The output o_i of the i-th neuron of a layer (starting from the second) is then

$$o_i = g_T\left(\sum_j \omega_{ij} o_j\right),$$

where the sum is made over the nodes of the previous layer.

[3]The sigmoid function squeeses the node output between 0 and 1; the final output becomes more peaked at 0 or 1 as the temperature decreases, becoming exactly 0 or 1 in the limiting case in which the temperature is zero.

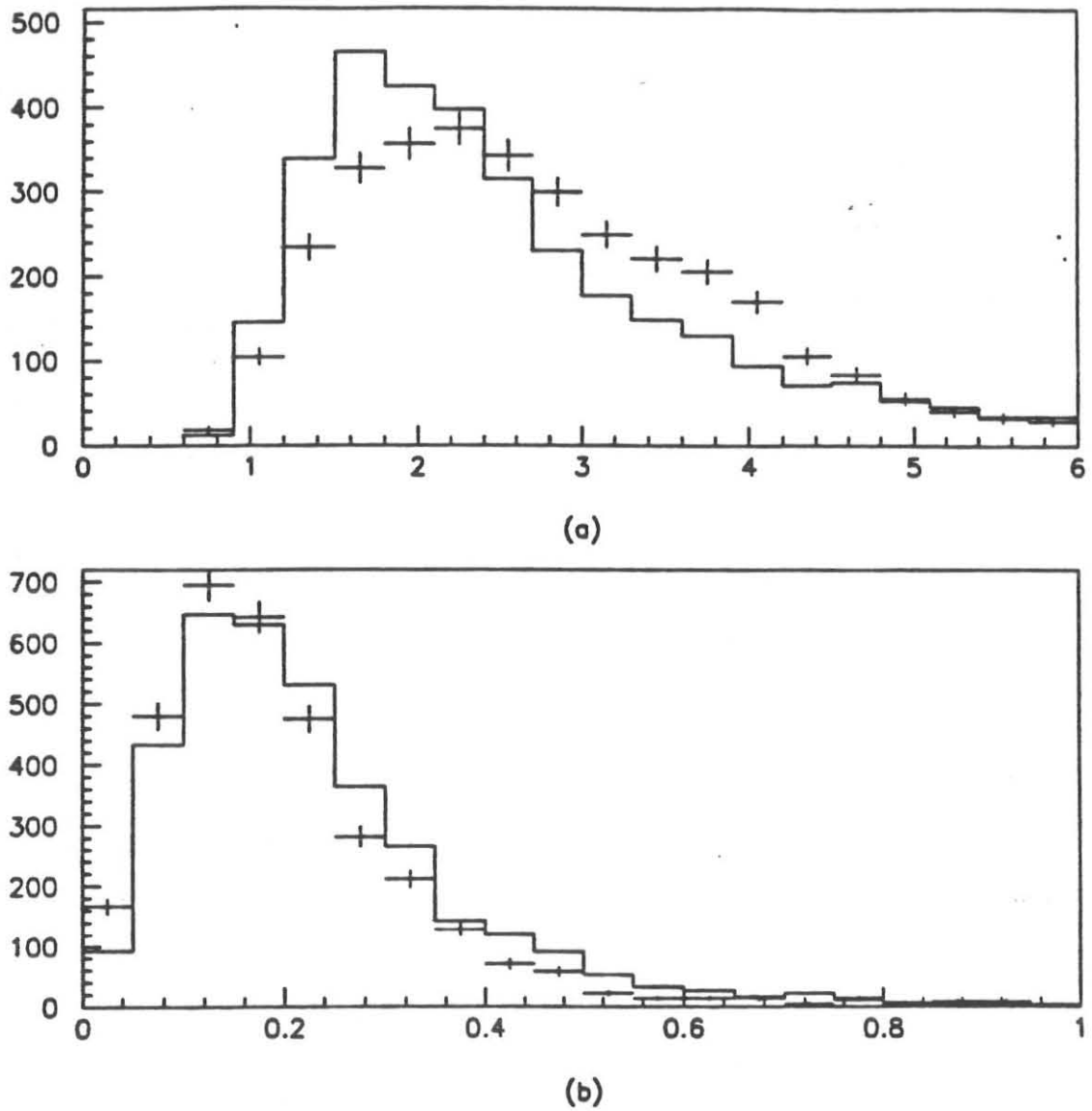

Figure 1: *Individual input variables (simulation). (a) Variable 4 (see text) for $b\bar{b}$ events (crosses), and for non-$b\bar{b}$ events (solid); (b) Variable 14 for $c\bar{c}$ events (crosses), and for non-$c\bar{c}$ events (solid). The distributions are normalized to the same area.*

The network training procedure fixes the values of the weights associated with the node interconnections. The aim is to realize a mapping of the input pattern space ($x_i \in$ P) to the feature space ($\Theta \in$ F), such that a good separation of events belonging to a class A from events belonging to the complementary class $\overline{A}$ is obtained by a simple cut in F.

In the "back-propagation" learning algorithm the output feature values obtained from the "training" input patterns are computed and compared with the corresponding desired "target" values. A least mean square error function E is computed to quantify the difference between the obtained output Θ and the desired target t.

$$E = \frac{1}{2} \sum_{patterns} (t - \Theta)^2 .$$

This function is minimized by changing ("updating") the weights by an amount computed from the error function by the gradient descent method [3]. The process is controlled by the "learning strength parameter" η and the "momentum" α [3]: each updating step in the space of weights, computed by gradient descent, is multiplied by η and added to the previous step, multiplied by α. To smooth out fluctuations, weights are updated using the cumulative error from a number of input training patterns (10 in our case). A sequence of 10 patterns will be simply called an "update" in the following.

For the training of the system, a set of 100,000 events generated by the Monte Carlo JETSET PS, plus a detector simulation, was used. The training was made with an equal number of "signal" (class A) and background (class $\overline{A}$) events, because it has been verified that this improves the performance of the network [6].

The training was done using the simulator JETNET [13] and the simulator developed in [6]. No differences in the performance were noted.

Two symmetric target values (0 for class A and 1 for class $\overline{A}$) were used.

At each step of the learning procedure, an indication on the performance of the network can be inferred from the error function. A more reliable evaluation is obtained by testing the response of the network on a set of input patterns independent of the training set. The test sample was generated by the Monte Carlo program JETSET PS, plus the full simulation of the detector DELSIM [12]. The test sample was made by 40,000 events.

The "signal efficiency" ϵ_S was measured as the ratio:

$$\epsilon_S = N_S^a / N_S ,$$

where N_S^a is the number of patterns accepted by the ($\Theta > \Theta_{cut}$) criterion in a sample of N_S input patterns of "A" type. The "purity" p was defined as:

$$p = N_S^a / [N_S^a + N_B^a] ,$$

where N_B^a is the number of patterns, accepted by the same criterion, from a sample of N_B background patterns. The purity can be interpreted as the fraction of "A"

	Network 1 ($u\bar{u}$+$d\bar{d}$)	Network 2 ($s\bar{s}$)	Network 3 ($c\bar{c}$)	Network 4 ($b\bar{b}$)
Nodes in the hidden layer	30	23	54	6
$T_{layer\ 1 \to layer\ 2}$	1.0	2.0	1.0	2.0
$T_{layer\ 2 \to layer\ 3}$	0.33	0.67	0.5	1.0
α (training)	0.5 - 0.8	0.5 - 0.8	0.1 - 0.9	0.5 - 0.9
η (training)	0.1 - 0.015	0.2 - 0.011	0.05 - 0.001	0.01 - 0.001

Table 1: Characteristics of the four neural networks

events to be found in a mixed sample, selected by the criterion $\Theta > \Theta_{cut}$, if the input events are a mixture of signal and background in the proportion predicted by the Standard Model.

In the training phase, the four networks were specialized in such a way that network "1" was designed to be more performant for separating Z^0 decays into $u\bar{u}$ or $d\bar{d}$, network "2" for separating decays into $s\bar{s}$ pairs, network "3" for separating decays into $c\bar{c}$ pairs, and network "4" for separating decays into $b\bar{b}$ pairs.

The architecture of each network is summarized in Table 1, together with the parameters used in the training phase. For the four neural networks, purity from the test sample is plotted versus efficiency in Fig. 2.

5. ANALYSIS AND RESULTS

From each of the four networks ($i = 1...4$), the fraction of events $\beta_j^{(i)}$ of each class j ($j = 1...4$) was determined by means of a χ^2 fit to the form

$$\Re^{(i)}(t) = \sum_j \beta_j^{(i)} a_j^{(i)}(t),$$

where $\Re^{(i)}(t)$ is the map of the data through the network i into the feature space, and $a_j^{(i)}(t)$ are the distributions for each class j in the feature space, determined in the test sample. All distributions were normalized to unity.

The four networks are constructed in such a way that each network provides a fit with small (in module) correlation coefficients between the class that the network itself was teached to distinguish and the other classes.

The determinations of the four branching fractions from each of the four networks are listed below, with the correlation coefficients $C^{(i)}$ from the fits. The four networks have been checked to be statistically independent inside the accuracy of the measurement.

$$\vec{\beta}^{(1)} = (0.455 \pm 0.034, 0.198 \pm 0.036, 0.155 \pm 0.041, 0.186 \pm 0.030)$$

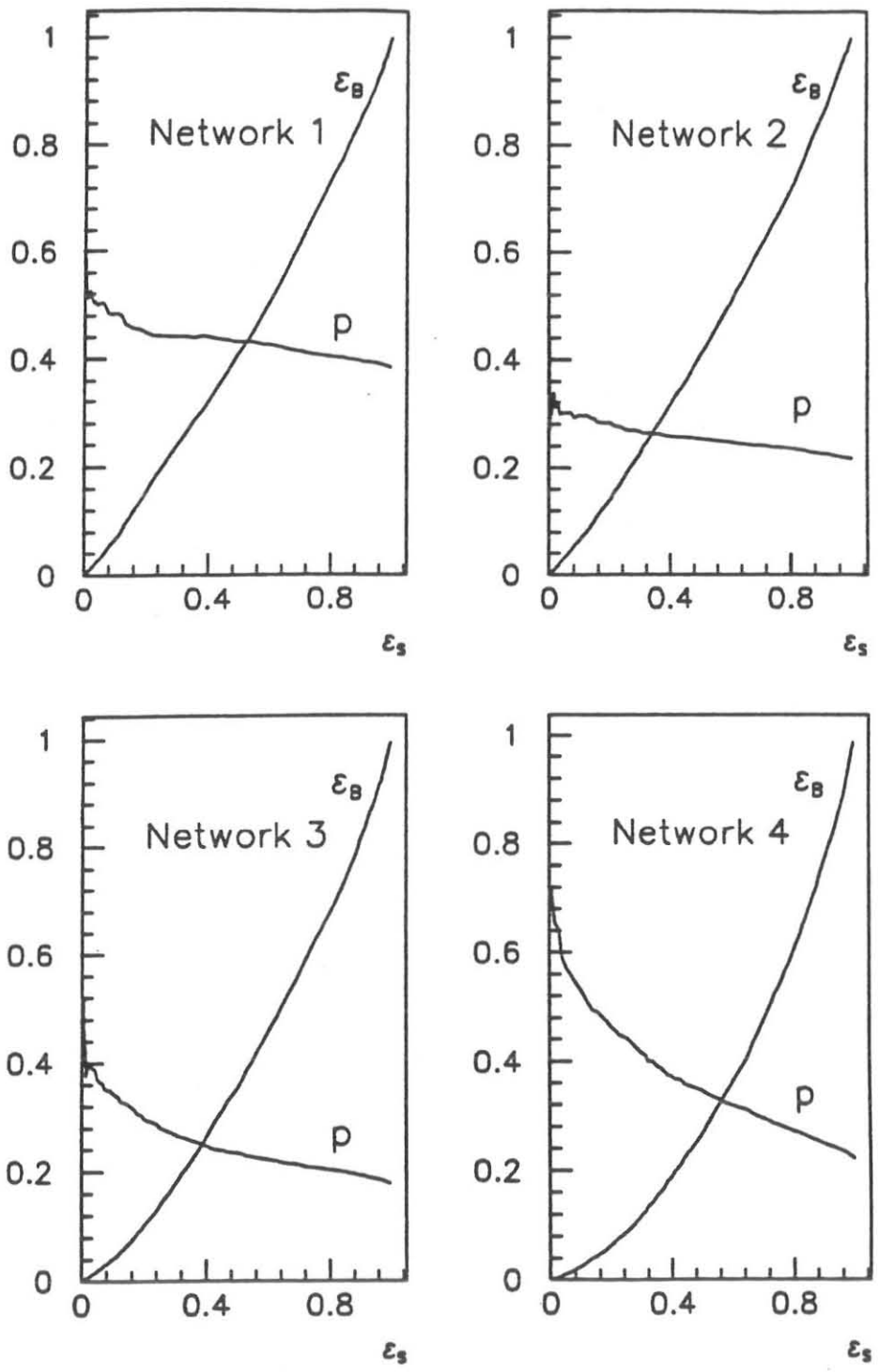

Figure 2: ***Purity of the sample selected and efficiency for background selection for each of the four networks, as a function of the efficiency for the selection of signal.***

$$C^{(1)} = \begin{pmatrix} 1.000 & -0.785 & -0.059 & -0.086 \\ -0.785 & 1.000 & -0.380 & 0.206 \\ -0.059 & -0.380 & 1.000 & -0.834 \\ -0.086 & 0.206 & -0.834 & 1.000 \end{pmatrix}$$

$$\chi^2_{(1)}/NDF = 122/(92-4)$$

$$\vec{\beta}^{(2)} = (0.421 \pm 0.036, 0.183 \pm 0.036, 0.198 \pm 0.046, 0.193 \pm 0.013)$$

$$C^{(2)} = \begin{pmatrix} 1.000 & -0.670 & -0.477 & -0.271 \\ -0.670 & 1.000 & -0.276 & 0.337 \\ -0.477 & -0.276 & 1.000 & -0.332 \\ -0.271 & 0.337 & -0.332 & 1.000 \end{pmatrix}$$

$$\chi^2_{(2)}/NDF = 122/(97-4)$$

$$\vec{\beta}^{(3)} = (0.435 \pm 0.052, 0.197 \pm 0.043, 0.104 \pm 0.015, 0.257 \pm 0.040)$$

$$C^{(3)} = \begin{pmatrix} 1.000 & -0.589 & -0.269 & -0.569 \\ -0.589 & 1.000 & -0.086 & -0.258 \\ -0.269 & -0.086 & 1.000 & 0.069 \\ -0.569 & -0.258 & 0.069 & 1.000 \end{pmatrix}$$

$$\chi^2_{(3)}/NDF = 130/(100-4)$$

$$\vec{\beta}^{(4)} = (0.411 \pm 0.056, 0.196 \pm 0.043, 0.180 \pm 0.043, 0.208 \pm 0.010)$$

$$C^{(4)} = \begin{pmatrix} 1.000 & -0.634 & -0.578 & -0.285 \\ -0.634 & 1.000 & -0.233 & 0.186 \\ -0.578 & -0.233 & 1.000 & -0.045 \\ -0.285 & 0.186 & -0.045 & 1.000 \end{pmatrix}$$

$$\chi^2_{(4)}/NDF = 115/(100-4)$$

A graphical output of the fits is displayed in Fig. 3.

Finally, the expression

$$\chi^2 \simeq \sum_i < \vec{\beta}^{(i)} - \vec{\beta}^* | C^{(i)-1} | \vec{\beta}^{(i)} - \vec{\beta}^* > ,$$

where $C^{(i)}$ is the covariance matrix in the fit from the i-th network, was minimized with respect to $\vec{\beta}^*$, under the constraint that the sum of the branching fractions is equal to 1. This leaded to the determinations

$$\begin{aligned} \Gamma_{u\bar{u}+d\bar{d}}/\Gamma_h &= 0.417 \pm 0.015 \\ \Gamma_{s\bar{s}}/\Gamma_h &= 0.233 \pm 0.016 \\ \Gamma_{c\bar{c}}/\Gamma_h &= 0.139 \pm 0.010 \\ \Gamma_{b\bar{b}}/\Gamma_h &= 0.211 \pm 0.006 , \end{aligned}$$

where the error quoted gives the size of the minimal hypercube that contains the error hyperellypse, and thus keeps into account correlations.

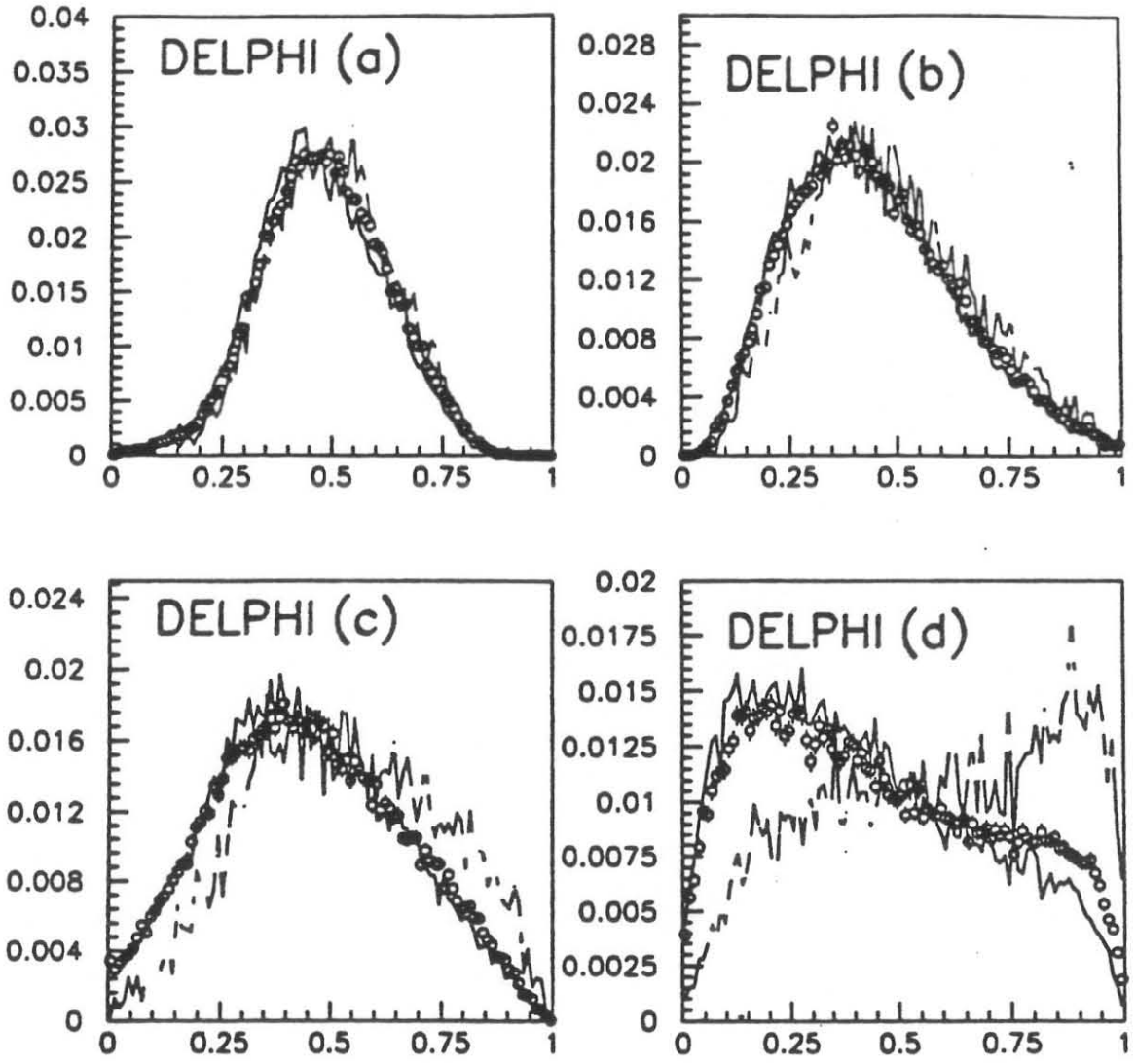

Figure 3: *Output of the four neural networks on real data (open circles), compared to the Monte Carlo predictions in the cases that the species on which the network is specialized is absent (solid line) or corresponds to the full sample (dashed line). Networks 1 (a), 2 (b), 3 (c), 4 (d).*

5.1 Study of Systematics

To study the systematics, the uncertainties in the best tuning of parameters in JETSET PS as parametrized in [10] were kept into account. In addition, a detailed study of the effect of fragmentation parameters was done.

Due to the amount of computer time required to provide a full simulation of events, systematics were studied by comparing approximate fast simulations with varying parameters (taken as "test data") with approximate fast simulations using JETSET PS with parameters tuned as in [10], taken as "real data".

The sources of systematic uncertainties which have been considered are listed below, and the effects are summarized in Table 2. The ranges of variation correspond to 1σ uncertainties, mainly from the determinations of [10].

1. $\Gamma_{u\bar{u}}/\Gamma_{d\bar{d}}$. The ratio between the branching fractions into $u\bar{u}$ pairs and the fraction into $d\bar{d}$ pairs is not known a-priori, and was assumed in the Monte Carlo as in the Standard Model. The effect of this assumption was checked by allowing a variation between a situation in which the $u\bar{u}$ events are completely absent and a situation in which the $d\bar{d}$ events are completely absent.

2. Λ. The parameter Λ in JETSET PS was allowed to vary between 0.28 and 0.31 GeV.

3. Q_0. The cutoff on the parton evolution was allowed to vary between 0.7 and 1.8 GeV.

4. Fragmentation. Systematic effects from fragmentation were checked:

   - In the Lund fragmentation scheme, by allowing a variation of the a parameter between 0.13 and 0.30 (the b parameter was fixed at 0.34 GeV^{-2}).
   - In the Peterson fragmentation scheme, by allowing a variation of ϵ_b between 2×10^{-3} and 7×10^{-3}, and a variation of ϵ_c between 15×10^{-3} and 40×10^{-3}.

   The average of the systematics in the two cases listed above was taken as estimator of the systematic uncertainty due to fragmentation.

5. γ_s/γ_u. A range of variation between 0.25 and 0.30 was allowed, consistent with the averages from [14].

6. $Br(D^{*\pm} \to D^0\pi^{\pm})$. A range of variation between 0.49 and 0.66 was allowed.

Comparisons with three different models for the decay of the Z^0 were tried: ARIADNE[15], HERWIG [16] and the JETSET Monte Carlo with QCD 2^{nd} order generation of the initial state at the parton level (JETSET ME). The Monte Carlos ARIADNE and HERWIG were tuned as in [10]; for JETSET ME, both the tunings suggested in [10] and [17] were used. In all cases, the comparison was impossible due

	$\Gamma_{u\bar{u}+d\bar{d}}/\Gamma_h$	$\Gamma_{s\bar{s}}/\Gamma_h$	$\Gamma_{c\bar{c}}/\Gamma_h$	$\Gamma_{b\bar{b}}/\Gamma_h$
$\Gamma_{u\bar{u}}/\Gamma_{d\bar{d}}$	=0.[illegible]	±0.020	±0.017	±0.001
Λ	=0.[illegible]	±0.016	±0.010	±0.015
Q_0	=0.[illegible]	±0.018	±0.044	±0.002
γ_s/γ_u	=0.[illegible]	±0.018	±0.016	±0.004
$Br(D^{*\pm} \to D^0\pi^\pm)$	=0.[illegible]	±0.008	±0.005	±0.001
Fragmentation	=0.[illegible]	±0.036	±0.028	±0.013
TOTAL	=0.[illegible]	±0.051	±0.058	±0.020

Table 2: Summary of systematic effects

to the fact that no values of the branching fractions were found for which the model could reproduce the data within a reasonable χ^2 (the cut was done at $\chi^2/NDF = 2$). This means that a better way of optimization of such Monte Carlos should be done before they are useful in such analysis.

A range of uncertainty at 68% CL between 0.32 and 0.40 GeV is assigned in [10] to the JETSET PS parameter σ_q, the transverse spread of the momentum of hadrons. This range appeared to be overestimated in the sense that, in the extreme values of the confidence interval, it was impossible to find a set of values for the branching fractions for which the network output could be fitted with a $\chi^2/NDF < 3$.

Due to the effect of systematics, the measurements become

$$\begin{aligned}
\Gamma_{u\bar{u}+d\bar{d}}/\Gamma_h &= [illegible]17 \pm 0.015 \pm 0.058 \\
\Gamma_{s\bar{s}}/\Gamma_h &= [illegible]33 \pm 0.016 \pm 0.051 \\
\Gamma_{c\bar{c}}/\Gamma_h &= [illegible]39 \pm 0.010 \pm 0.058 \\
\Gamma_{b\bar{b}}/\Gamma_h &= [illegible]11 \pm 0.006 \pm 0.020 .
\end{aligned}$$

These results, using the determination of the hadronic partial width of the Z^0 given by DELPHI [18], $\Gamma_h = 1726 \pm 19$ MeV, provide

$$\begin{aligned}
\Gamma_{u\bar{u}+d\bar{d}} &= [illegible]20 \pm 104\,\text{MeV} \\
\Gamma_{s\bar{s}} &= [illegible]92 \pm 91\,\text{MeV} \\
\Gamma_{c\bar{c}} &= [illegible]40 \pm 102\,\text{MeV} \\
\Gamma_{b\bar{b}} &= [illegible]64 \pm 35\,\text{MeV} .
\end{aligned}$$

5.2 Separation of $u\bar{u}$ from $d\bar{d}$

Photon bremsstrahlung from quarks allows a fifth independent equation relating the hadronic branching fractions of the Z^0. The cross section for this process is approximately independent of the quark masses in the region of high p, high p_t of the emitted photon, but is proportional to the square of the charge of the quark.

From the average of Ref. [19], one obtains

$$\Gamma_{u\bar{u}}/\Gamma_h + \Gamma_{c\bar{c}}/\Gamma_h = 0.44 \pm 0.08$$

that, together with the determinations of the hadronic branching fractions of the four classes separated by the networks, gives

$$\begin{aligned} \Gamma_{u\bar{u}}/\Gamma_h &= 0.30 \pm 0.10 \\ \Gamma_{d\bar{d}}/\Gamma_h &= 0.12 \pm 0.10\,. \end{aligned}$$

The errors quoted above are of course almost completely anticorrelated.

6. CONCLUSIONS

The first determination in the literature of the hadronic branching fractions of the Z^0 boson into all five known quarks has been presented. To the knowledge of the authors, this is also the first time that results on a taxonomy problem have been obtained in high-energy physics using neural networks.

The results on all branching fractions are consistent with the predictions of the Standard Model.

Neural networks have shown the potentiality of a powerful tool for classification. The errors quoted will substantially decrease when variables related to impact parameters and lepton spectrum will be used as additional inputs [6].

The study of the effect of changing the Monte Carlo model used for computing efficiencies will require a more complete work of optimization of the other models available.

Acknowledgements

We are greatly indebted to our technical staffs and collaborators and funding agencies for their support in building the DELPHI detector and to the many members of the LEP division for the excellent performance of the LEP machine.

This work was supported by the Ministero dell'Universita' e della Ricerca Scientifica e Tecnologica, Rome (Italy).

References

1. J. Carter, Talk at the Plenary Session of the 1991 LP-HEP Conference, Geneva, July 1991.
2. P. Roudeau, Talk at the Plenary Session of the 1991 LP-HEP Conference, Geneva, July 1991.
3. D.E.Rumelhart, G.E.Hinton and R.J.Williams, "Learning Internal Representations by Error Propagation", in D.E.Rumelhart and J.L.McLelland (Eds.), "Parallel Distributed Processing: Explorations in the Microstructure of Cognition (Vol.1)", MIT Press (1986).
4. L. Lönnblad et al., *Nucl. Phys.* **B349** (1991) 675.
5. R. Marshall, *Z. Phys.* **C26** (1984) 291.
6. C. Bortolotto, A. De Angelis and L. Lanceri, UDPHIR 89/06/AA (Udine, December 1990), to be published in Nucl. Instr. and Meth. A.
   L. Bellantoni et al., CERN-PPE/91-80, May 1991.
   P. Henrard (ALEPH Coll.), presented at the 4th Symposium on Heavy Flavour Physics, Orsay, June 1991.
7. P. Aarnio et al. (DELPHI Coll.), *Nucl. Instr. and Meth.* **A303** (1991) 233.
8. P. Aarnio et al. (DELPHI Coll.), *Phys. Lett.* **B240** (1990) 271.
9. T. Sjöstrand, Comp. *Phys. Comm.* **27** (1982) 243, ibid. **28** (1983) 229.
   T. Sjöstrand and M. Bengtsson, *Comp. Phys. Comm.* **43** (1987) 367.
10. M.Z. Akrawy et al. (OPAL Coll.), *Z. Phys.* **C47** (1990) 505.
11. W. Bartel et al. (JADE Coll.), *Z. Phys.* **C33** (1986) 23.
12. DELSIM User's Guide, DELPHI 89-67 PROG 142, Geneva, July 1989.
    DELSIM Reference Manual, DELPHI 89-68 PROG 143, Geneva, September 1989.
13. L. Lönnblad, et al., *Phys. Rev. Lett.* **65** (1990) 1321.
14. G. Alexander et al. (OPAL Coll.), CERN-PPE/91-86, May 1991.
    DELPHI Coll., contribution to the 1991 LP-HEP Conference, Geneva, July 1991.
15. L. Lönnblad, LU TP 90-10, Lund 1990.
16. G. Marchesini and B.R. Webber, *Nucl. Phys.* **B238** (1984) 1.
17. W. de Boer, H. Fürstenau and J. Köhne, *Z. Phys.* **C49** (1991) 141.
18. P. Abreu et al. (DELPHI Coll.), CERN-PPE/91-95, May 1991.
19. G. Alexander et al. (OPAL Coll.), CERN-PPE/91-81, May 1991.
    DELPHI Coll., contribution to the 1991 LP-HEP Conference, Geneva, July 1991.